



NRL/MR/6110--02-8650

Frequency-Domain Electromagnetic Induction Sensors for the Multi-sensor Towed Array Detection System

H. H. NELSON

*Chemical Dynamics and Diagnostics Branch
Chemistry Division*

B. BARROW

T. BELL

R. S. JONES

*AETC, Incorporated
Arlington, VA*

B. SANFILIPPO

I. J. WON

*Geophex, Limited
Raleigh, NC*

November 27, 2002

20030109 171

Approved for public release; distribution is unlimited.

REPORT DOCUMENTATION PAGE				Form Approved OMB No. 0704-0188	
Public reporting burden for this collection of information is estimated to average 1 hour per response, including the time for reviewing instructions, searching existing data sources, gathering and maintaining the data needed, and completing and reviewing this collection of information. Send comments regarding this burden estimate or any other aspect of this collection of information, including suggestions for reducing this burden to Department of Defense, Washington Headquarters Services, Directorate for Information Operations and Reports (0704-0188), 1215 Jefferson Davis Highway, Suite 1204, Arlington, VA 22202-4302. Respondents should be aware that notwithstanding any other provision of law, no person shall be subject to any penalty for failing to comply with a collection of information if it does not display a currently valid OMB control number. PLEASE DO NOT RETURN YOUR FORM TO THE ABOVE ADDRESS.					
1. REPORT DATE (DD-MM-YYYY) November 27, 2002		2. REPORT TYPE Interim Report		3. DATES COVERED (From - To) March 2000-January 2002	
4. TITLE AND SUBTITLE Frequency-Domain Electromagnetic Induction Sensors for the Multi-sensor Towed Array Detection System				5a. CONTRACT NUMBER W74RDV10093316	
				5b. GRANT NUMBER	
				5c. PROGRAM ELEMENT NUMBER	
6. AUTHOR(S) H.H. Nelson, B. Barrow,* T. Bell,* R.S. Jones,* B. SanFilipo,† and I.J. Won†				5d. PROJECT NUMBER	
				5e. TASK NUMBER	
				5f. WORK UNIT NUMBER 61-5802-E1	
7. PERFORMING ORGANIZATION NAME(S) AND ADDRESS(ES) Naval Research Laboratory, Code 6110 4555 Overlook Avenue, SW Washington, DC 20375-5320				8. PERFORMING ORGANIZATION REPORT NUMBER NRL/MR/6110--02-8650	
9. SPONSORING / MONITORING AGENCY NAME(S) AND ADDRESS(ES) Environmental Security Technology Certification Program 901 North Stuart Street Suite 303 Arlington, VA 22203				10. SPONSOR / MONITOR'S ACRONYM(S) ESTCP	
				11. SPONSOR / MONITOR'S REPORT NUMBER(S)	
12. DISTRIBUTION / AVAILABILITY STATEMENT Approved for public release; distribution is unlimited.					
13. SUPPLEMENTARY NOTES *AETC, Inc., Arlington, VA 22202 †Geophex, Ltd., Raleigh, NC 27603					
14. ABSTRACT The Chemistry Division of the Naval Research Laboratory has developed the Multi-sensor Towed Array Detection System for use in unexploded ordnance detection and classification. With support from the Environmental Security Technology Certification Program, we are developing a frequency-domain electromagnetic induction sensor array to extend our capabilities. The first task in this program is to characterize the commercial GEM-3 sensor and assess its suitability for use in a towed array. In this report, we detail our characterization results and note the problems we encountered. We conclude by listing the modifications to the baseline sensors that we will make for the array we will field.					
15. SUBJECT TERMS Multi-sensor Towed Array Detection System (MTADS); Electromagnetic induction; Unexploded ordnance (UXO)					
16. SECURITY CLASSIFICATION OF:			17. LIMITATION OF ABSTRACT UL	18. NUMBER OF PAGES 19	19a. NAME OF RESPONSIBLE PERSON Herbert H. Nelson
a. REPORT Unclassified	b. ABSTRACT Unclassified	c. THIS PAGE Unclassified			19b. TELEPHONE NUMBER (include area code) (202) 767-3686

CONTENTS

FIGURES	iv
TABLE	iv
INTRODUCTION	1
RESULTS	2
Issues to be Investigated	2
Single Sensor Tests	3
GEM-3	3
GEM-5	6
GEM-3 Arrays	8
Non-Synchronous Simultaneous Array	8
Non-synchronous Sequential Array	9
Array Noise Investigation	12
SENSOR SPECIFICATION FOR DEMONSTRATION ARRAY	14
REFERENCES	15

FIGURES

Figure 1. Schematic representation of the two sensor configurations	2
Figure 2. GEM-3 sensor on the Blossom Point test stand.....	3
Figure 3. Response of the baseline GEM-3 to a standard aluminum sphere	4
Figure 4. Derived response coefficients for a steel cylinder	4
Figure 5. Calculated depth dependence of GEM-3 response	5
Figure 6. Walking survey noise from the baseline GEM-3	6
Figure 7. Comparison of static noise from GEM-3 and GEM-5	6
Figure 8. GEM-5 survey noise at two frequencies.....	7
Figure 9. GEM-3 crosstalk as a function of sensor separation.....	8
Figure 10. GEM-3 array on test cart	9
Figure 11. Calibration of individual sensors in the array	10
Figure 12. Static and dynamic characterization of the GEM-3 array	10
Figure 13. Comparison of static vs. walking noise	11
Figure 14. Peak frequency of the quadrature response as a function of target diameter	11
Figure 15. Quantification of the static vs. dynamic noise amplitude	12
Figure 16. Sketch of the proposed GEM-3 array	14

TABLE

Table 1. Initial schedule for sensor characterization tests.....	3
--	---

FREQUENCY-DOMAIN ELECTROMAGNETIC INDUCTION SENSORS FOR THE MULTI-SENSOR TOWED ARRAY DETECTION SYSTEM

INTRODUCTION

Unexploded Ordnance (UXO) detection and remediation is a high priority triservice requirement. Current estimates suggest that there are nearly 6 million acres of Closed, Transferred, and Transferring Ranges contaminated with UXO. The projected cost to remediate these lands ranges from \$10 to \$100B. These cost estimates are based on remediation using the traditional "mag and flag" method. This technique is slow, labor intensive, and inefficient; upwards of 70% of the costs of a typical "mag and flag" survey go to removal of non-UXO items and investigation of "dry holes." There has been considerable progress in the detection of buried UXO in the last seven years. The Multi-sensor Towed Array Detection System (*MTADS*), supported by the Environmental Security Technology Certification Program (ESTCP), has demonstrated detection capability for all military ordnance to its maximum self-burial depth¹ with location accuracies² on the order of 15 cm. Discrimination of UXO from ordnance fragments and other clutter remains as a problem, however. We have shown that with careful mission planning and a modest on-site training effort, an *MTADS* survey/remediation project can achieve false alarm rates substantially lower than those quoted for "mag and flag" surveys. However, there is still much room for improvement in discrimination ability that will result in direct reduction of remediation costs.

The Chemistry Division of the Naval Research Laboratory has participated in several programs funded by SERDP and ESTCP whose goal is to enhance the discrimination ability of *MTADS*. The process is based on making use of both the location information inherent in an item's magnetometry response and the shape and size information inherent in the response to the time-domain electromagnetic induction sensors that are part of the baseline *MTADS* in either a cooperative or joint inversion. We have already made significant progress toward our goal. The algorithms and methods that were developed for the ESTCP program involving analysis of data from the *MTADS* EM61 array were applied in preliminary form at the JPG-IV Demonstration allowing us to score as one of the small group of approaches that showed any classification ability.³ More recently, we have used the methods at JPG-V and on a live range, the Impact Area of the Badlands Bombing Range, SD. In all these demonstrations, our classification ability has been limited by the information available from the sensor. The EM61 is a time-domain instrument with a single gate to sample the amplitude of the decaying signal. To make further progress on UXO classification, a sensor with more information available is required.

By far the best results at JPG-IV were obtained by Geophex and AETC using magnetometers and the GEM-3 frequency-domain electromagnetic induction sensor.⁴ The GEM-3 sensor is a frequency-domain sensor with at least ten frequencies available for simultaneous measurement of the in-phase and quadrature response of the target. Thus, in principle, there is much more information available from a GEM-3 sensor for use in classification decisions. Unfortunately, the commercial GEM sensor is a hand-held instrument with relatively slow data rates and is thus not very amenable to rapid, wide area surveys. ESTCP Project 200033, Enhanced UXO Discrimination Using Frequency-Domain Electromagnetic Induction, has been funded to overcome this limitation by integrating an array of GEM sensors with the

MTADS platform. One of the first tasks in this program is to specify the sensor configuration that will result in an acceptable survey rate when configured as an array while retaining the classification performance of the hand-held GEM-3. This report summarizes the results of the sensor specification task.

RESULTS

Issues to be Investigated

The program plan for the ESTCP program specified a two-part investigation of sensor choices. In part 1, a thorough investigation of the baseline GEM-3 sensor was to be carried out. Issues such as response, drift, system noise, etc. were to be investigated. Following this, possible modifications to the system were to be considered.

As early as the time of the proposal for the program, it was recognized that the GEM-3 planar arrangement was not ideal for array deployment. The GEM-3 relies on a bucking coil to cancel the transmit field at the receive coil and thus achieve the part-per-million sensitivity required. When two, or more, GEM-3 sensors are placed in close proximity, the transmit field from one sensor is incompletely cancelled at the receive coil of the other. Given unlimited dynamic range in the sensor, this would be no problem. For real-world sensors however, this can lead to saturation and loss of sensitivity. One proposal from Geophex was to consider a co-axial, gradiometric sensor for use in an array. Both of these configurations are shown schematically in Figure 1.

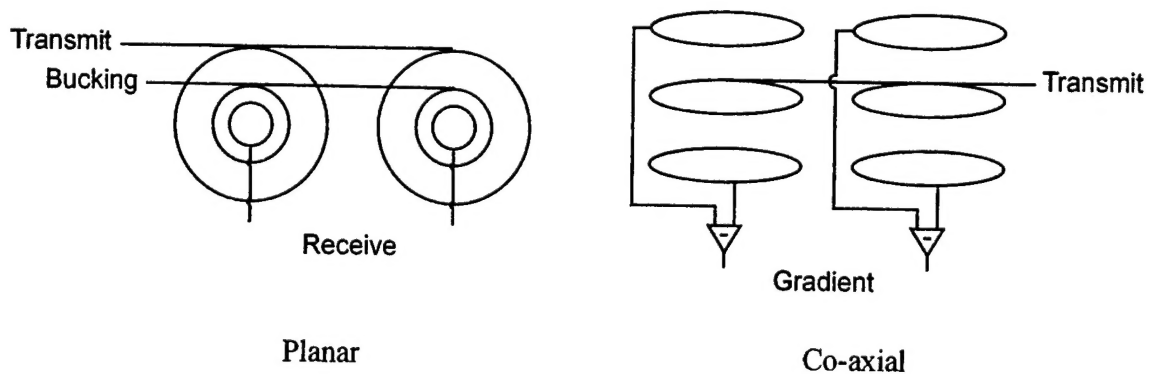


Fig. 1 – Schematic representation of the proposed sensor configurations. The planar configuration, shown on the left, is the traditional GEM-3 configuration.

For either of the possible configurations shown above, the issue of inter-sensor timing must be addressed. The original *MTADS* EM61 array is run synchronously; all three sensors are triggered by a common pulse. This has the advantage of producing a large transmit moment and thus good depth sensitivity but it reduces the number of independent interrogation angles available from a single pass of the array. This synchronous transmission of the primary field using all three (overlapping) transmit coils is effectively transmitting with a single loop (superposition) having cross-track size large (2 m) compared to the depths of most of the UXO of concern, and the same width as the survey line-spacing. Targets that are under the central region of the array (i.e. not under the array lateral edge) are illuminated with fields that rotate from horizontal in the down-track direction to vertical and back to horizontal down-track as the array passes, but are not illuminated horizontally across-track. If the individual coils are sequenced (transmitting one after the other), targets that are directly below one transmit coil will be illuminated by the adjacent coil from the cross-track direction.

For the GEM array, we want the sensors to be independent units to maximize our "looks" at the target. Given this, the sensors can be triggered simultaneously or sequentially. Simultaneous operation increases the data rate from each sensor but is susceptible to the sensor cross-talk problems mentioned above. Sequential triggering eliminates the cross-talk problem but may place unacceptable limitations on survey speed. To examine all these effects, a matrix of sensor tests was scheduled at the Geophex facility and NRL's Blossom Point Test Site in Calendar 2000 and early 2001. The initial schedule is shown in Table 1. Here, non-synchronous simultaneous operation refers to an array in which the sensors are operating independently; i.e. with no known or controlled phase relation.

Table 1 — Initial Schedule for Sensor Characterization Tests

	Single Sensor	Non-synchronous Simultaneous Array	Non-synchronous Sequential Array
Planar	May, 2000 Blossom Point	July, 2000 Geophex Facility	January, 2001 Blossom Point
Co-Axial	December, 2000 Blossom Point		February, 2001 Blossom Point

Single Sensor Tests

GEM-3

The baseline GEM-3 sensor was characterized at the Blossom Point Test Facility⁵ in May 2000. Both static tests on our sensor test stand, Figure 2, and walking tests over the ordnance classification test site were carried out. On the test stand, data were collected as a function of distance from sensor, orientation,

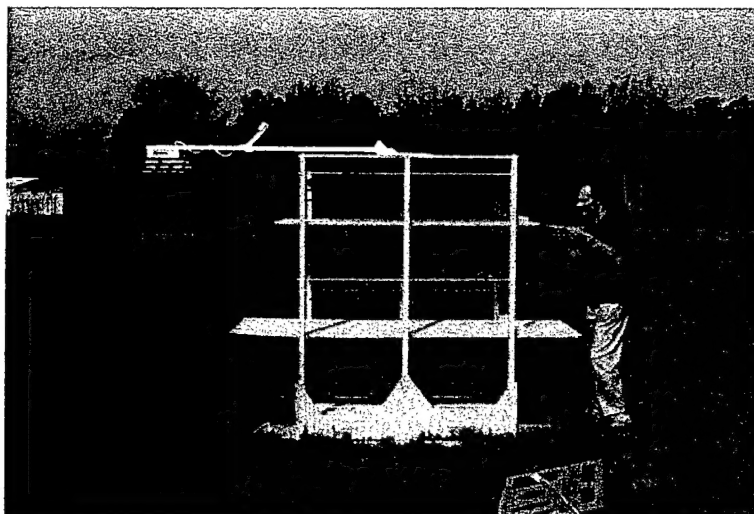


Fig. 2 – GEM-3 sensor mounted on a test stand at Blossom Point

and position for a suite of test objects including standard spheres and cylinders and some small ordnance items. The baseline GEM-3 sensor is available with three coil sizes, 40-cm, 64-cm, and 96-cm diameter. All three coils were used in these tests.

The first measurement conducted when a new sensor is to be characterized is the sensor's response to a test sphere. This response can be calculated analytically and thus provides a good test of sensor performance. The measured response of the baseline GEM-3 to a standard 4-in diameter aluminum sphere 48 cm below the sensor is shown in Figure 3 both as a function of excitation frequency and of position under the sensor for a specific frequency. PPM in the right panel refers to the fraction of the transmit current that is induced in the receive coil. The calculated response is plotted as the solid line in the figure. As can be seen, there is excellent agreement between the measured and calculated response.

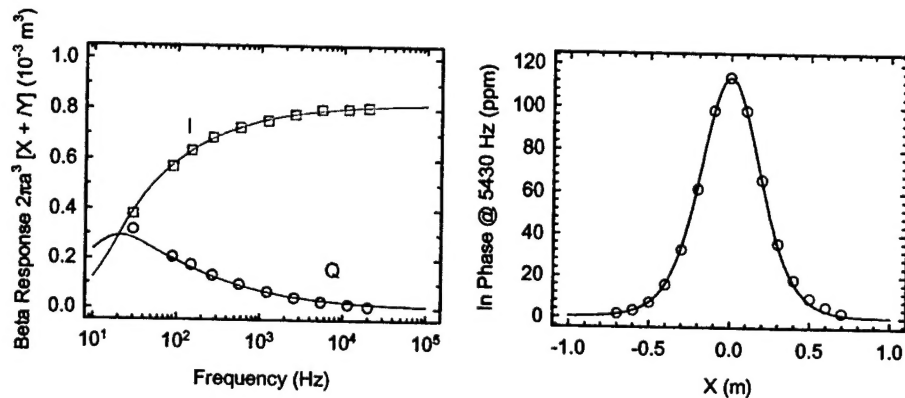


Figure 3 – Response of the baseline GEM-3 to a standard 3-in diameter aluminum test sphere 48 cm below the sensor. The left plot shows the in-phase and quadrature response as a function of excitation frequency and the right plot shows the response as a function of position at 5430 Hz. The measured response is shown as symbols and the calculated response as a solid line.

The relative performance of the three available coil sizes is shown in Figures 4 and 5. In Figure 4, the target response coefficients, β , of a test steel cylinder for both longitudinal and transverse excitation are plotted as a function of frequency. To derive these coefficients, measurements were made with the test cylinder oriented vertically and horizontally directly under the sensor. Target distance from the sensor was 48 cm for the smallest coil and 94 cm for the two largest coils. The derived response coefficients agree quite well for each of the three sensor coils; the main deviation is for the quadrature response at low frequencies where the signal is low and sensor noise is an issue.

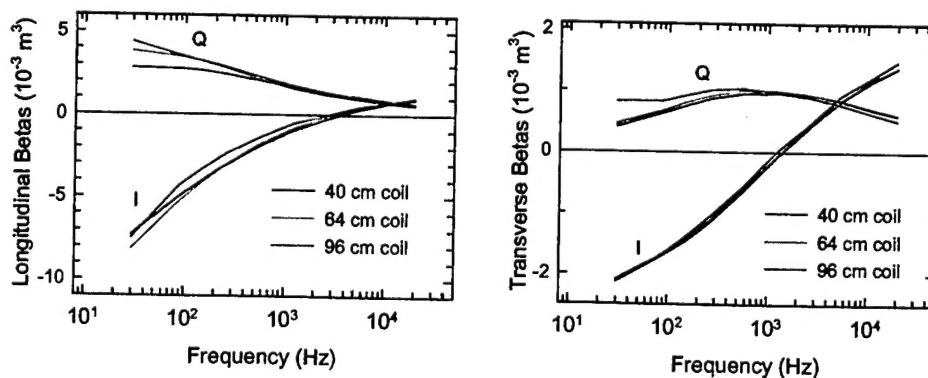


Figure 4 – Derived response coefficients for a 3- x 12-in steel cylinder after excitation by a GEM-3 with three different coil sizes. The longitudinal response as a function of frequency is plotted on the left and the transverse response on the right.

There are obviously trade-offs among the coil sizes for use in UXO discrimination. The larger coils have larger transmit moments so they are able to detect deeper targets. This is illustrated in Figure 5. This figure plots the response of the GEM-3 with each of the available coil sizes to a hypothetical target as a function of the depth of the object below the sensor. The "sensor output" plotted is the dot product between the primary field generated by the transmit coil (accounting for finite loop size and number of turns as well as bucking coil) and one that would be generated by the receive coil if it were transmitting (normalized to unity current). This represents the net sensor inductive coupling to a point in space and is independent of target, and is meant to characterize EMI sensor configurations without regard to a specific target in terms of sensitivity to target location. In fact, it is equivalent to the in-phase response to a small (compared to coil sizes and target distance), perfectly conducting sphere (normalized by the sphere radius cubed). A reference line is shown at a sensor output of 10 ppm, which we have found to be the minimum output with acceptable S/N for discrimination based on the reproducibility of spectra such as those shown in Figure 4 for signals above and below that threshold. As can be seen, the 96-cm diameter coil can classify this object to a depth of 1 m below the coil while the smallest coil is only useful to a depth of 65 cm below the coil. On the other hand, the smaller coil gives better target location information.

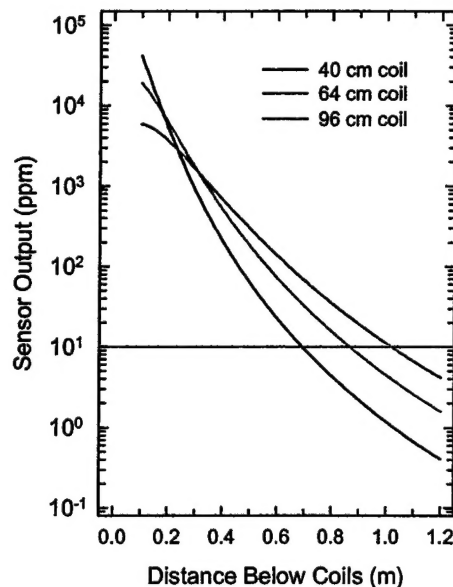


Figure 5 – Calculated sensor response to a hypothetical target as a function of depth below the sensor for each of the three available coil sizes. The reference line marks the lowest output for which reliable classification is possible.

The final test in our initial characterization of the baseline GEM-3 sensor was a short walking survey of our ordnance classification test site. For this test, the sensor was hand-carried on successive back-and-forth traverses of the top 20 meters of the test field. The results of this measurement are shown in Figure 6. The vertical scale of the plots are chosen to allow examination of the sensor noise at each of five frequencies; the target responses are off scale. The measured noise is approximately equal at frequencies from 30 Hz to 20 kHz.

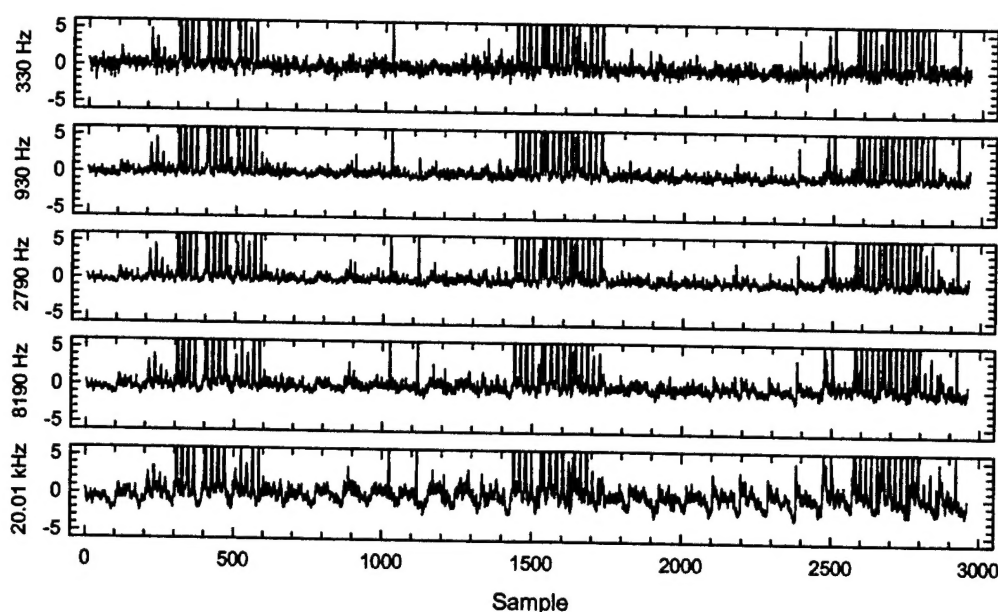


Figure 6 – Results of a walking survey of a portion of the test field at Blossom Point

GEM-5

Geophex, Ltd. Designed and built a prototype co-axial instrument (Figure 1) that they termed the GEM-5. Initial characterization measurements on this new sensor were carried out at the Geophex facility in Raleigh, NC. Figure 7 shows a comparison of the standard GEM-3 vs. this prototype GEM-5 static S/N ratio for a steel cylinder at several depths and frequencies. Briefly, the parameters of the prototype GEM-5 are: coil radii (Tx and Rx) = 25 cm, Tx-Rx separation = 35cm, 60 Rx turns, 9 Tx turns. The electronics are as in the GEM-3, without coil embedded preamplifier; custom passive circuit tuning of coils is incorporated into each. As can be seen from the figure, in all cases the GEM-3 shows superior S/N performance.

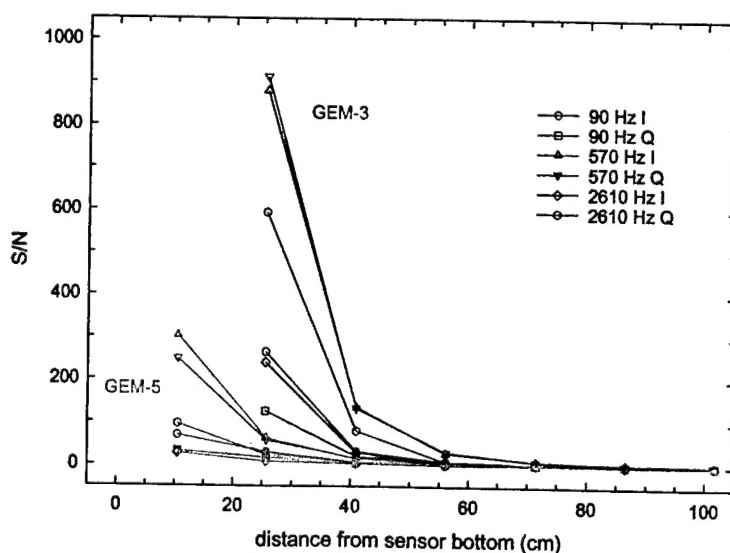


Figure 7 – Comparison of static signal to noise as a function of frequency and object distance from the sensor for a GEM-3 vs. the prototype GEM-5

Of more relevance to the current program is dynamic noise. Figure 8 depicts a small portion of a survey over three seeded targets (left-to-right along profile a 2.5"x12" steel pipe oriented cross-track at 45° inclination, buried 0.6 m to center; a 3.1"x18" steel pipe, vertical orientation, buried 0.7 m to center; and a 2.5"x12" steel pipe oriented horizontal along-track, buried 0.6 m to center) in the Geophex backyard. The prototype GEM-5 was mounted on a small cart with the lower receive coil approximately 15 cm above the ground and pushed over the targets. Data collected at 150 Hz and 5430 Hz are plotted in the figure. The GEM-5 data quality degraded less with bouncing motion than did the GEM-3s in our prototype array, but, as Figure 7 shows, the GEM-3 noise characteristics are sufficiently superior to overcome this advantage. The three targets are clearly evident in the 5430 Hz data but the noise at 150 Hz makes it difficult to reliably detect more than one of the targets. These results corroborate those shown in Figure 7, the S/N ratio of the prototype GEM-5 is lower than the baseline GEM-3.

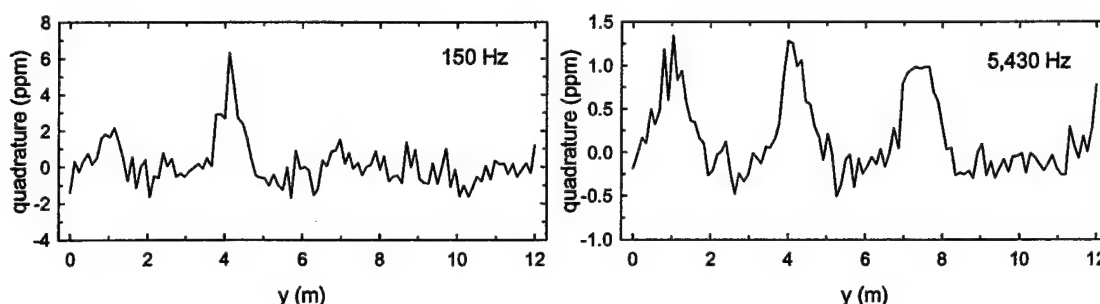


Figure 8 – Comparison of the survey noise from the prototype GEM-5 at two frequencies

Even with this lower S/N, the co-axial arrangement is attractive because its gradiometric configuration offers the possibility of cancellation of the transmit field of adjacent sensors. Of course, success of this cancellation requires dimensional rigidity of the sensors in the array. We performed a simple analysis of the rigidity required and found that for relative displacements of 0.1 mm the uncanceled crosstalk would exceed the signal expected for an 81-mm mortar buried at 35 cm.⁶ For this analysis we assume the transmit and receive coils are dipoles (note that in the model, a transmit radius of 7.5 cm with 10 turns, 3 A current was used for computing a moment, but the field equations were dipolar, and the moment cancels since both signal and crosstalk are proportional to moment), transmit-receive separation of 15 cm, horizontal separation of array members of 25 cm, and the bottom receive coil 25 cm above ground (the 35 cm depth of burial is measured from ground surface, so that total distance is 60 cm). The analysis approach was simply to compute the cross talk for vertical displacement of one coaxial sensor transmit coil relative to the adjacent sensor receive pair and compare the unbuckled primary field to that of the target response, based on actual GEM-3 empirical data for the 81 mm ordnance. While this estimate is for arbitrary GEM-5 parameters, not those of a future array, it became clear that the GEM-5 sensor requires more development and is not appropriate for a 6.4 Demonstration/Validation program. We thus narrowed the focus of our investigation to the GEM-3 and its variants.

GEM-3 Arrays

Non-Synchronous Simultaneous Array

As originally planned, this issue was investigated at the Geophex facility in July 2000. The objective was to quantify the level of "cross-talk" primary field interference between adjacent coplanar GEM-3 sensors operating independently (i.e. non-synchronously) and simultaneously. In particular, it was of interest to determine the sensor separation at which saturation occurs, because that would preclude synchronous simultaneous operation at that separation without changing the electronics or coil moments.

Two GEM-3 sensors with 40 cm diameter disks, with one serving as the primary sensor and the second transmitting during alternate recording sequences to induce an interfering transmit field, were configured to operate in multifrequency mode (hybrid waveform) at 330, 930, 2790, 8190, and 20010 hertz, with one 30 Hz base period per data sample, in a continuous (survey) operation. The sensors were placed on wooden stands in nominally level, coplanar geometry at different offset distances ranging from 3.75 m down to 1.25 m center to center. At each distance, four data sweeps (recorded as line #'s) were recorded, first with the second GEM not transmitting, then with it transmitting, followed by repeats of each. Data were recorded remotely to a personal computer over an RS-232 serial link. Sensor spacing was determined using a measuring tape taped in a fixed position onto the primary GEM; the tape was non-metallic except for the end hook, which was left hanging inside the receive loop, serving as a small close-range target. The final sweep was taken with the target removed for comparison with the interfering signal levels. Also, a sweep was recorded with the second GEM at close range but not transmitting, followed by a sweep with the second GEM removed from the area in order to get a preliminary measure of the passive response of an adjacent GEM. The results of one such measurement at 330 Hz is shown in Figure 9.

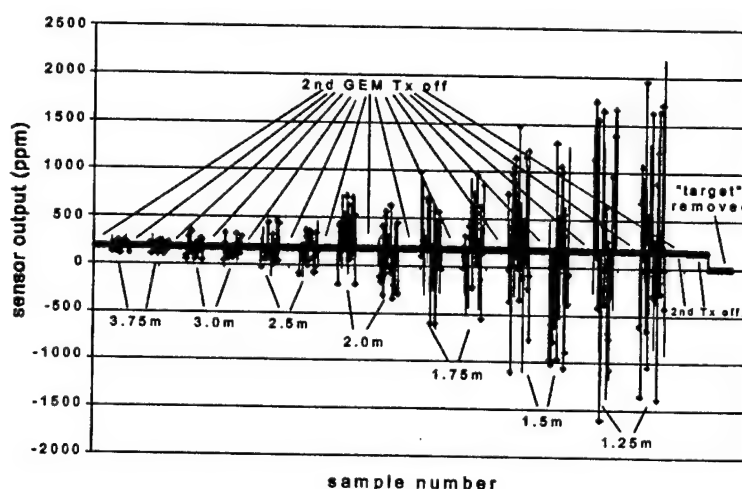


Fig. 9 – Results of a measurement of crosstalk between adjacent, simultaneously operating GEM-3s as a function of sensor separation

Even at a separation of 3.75 m, the largest tested, the interfering signal from the second GEM is on the order of 100 ppm. As mentioned above, the lowest useful signal from these sensors for classification purposes is ~10 ppm. Thus, the interference is large even at extremely large separations. Even worse, at separations below 1.75 m, the interference exceeds the sensor's A/D dynamic range and the output is flagged as saturated. In addition to the large amplitude, the phase of the interference is random, reflecting

the non-synchronous operation of the two sensors. This makes it unlikely that a cancellation scheme could be successfully employed to deal with this interference.

From these measurements, we conclude that autonomous GEM-3 sensors cannot simply be mounted on a platform as a towed array because of the mutual unbuckled interfering primary fields. Even if the sensors could be synchronized so that in principle the "cross-talk" primary fields were repeatable with fixed phase and could be calibrated, with the existing electronics, the A/D dynamic range would be exceeded at practical sensor separations. All further effort will be focussed on a sequential array.

Non-synchronous Sequential Array

A non-synchronous, sequential array of three GEM-3 sensors was constructed and mounted on a small cart for testing at Blossom Point. It is shown in Figure 10. For this test article 40-cm diameter coils were chosen for convenience; this was not required. The coil spacing was 0.5 m center-center. This was chosen to ensure that for all targets of interest we would obtain a response from more than a single sensor, which is necessary to resolve the position, orientation, and dipole beta response (response along three principle axes) of the target. It is a practical separation for trade-off between special resolution and production rates. Inter-sensor timing is controlled by the electronics package shown on the back of the cart. Data are recorded in a notebook computer that is located on the cart handle visible to the operator.

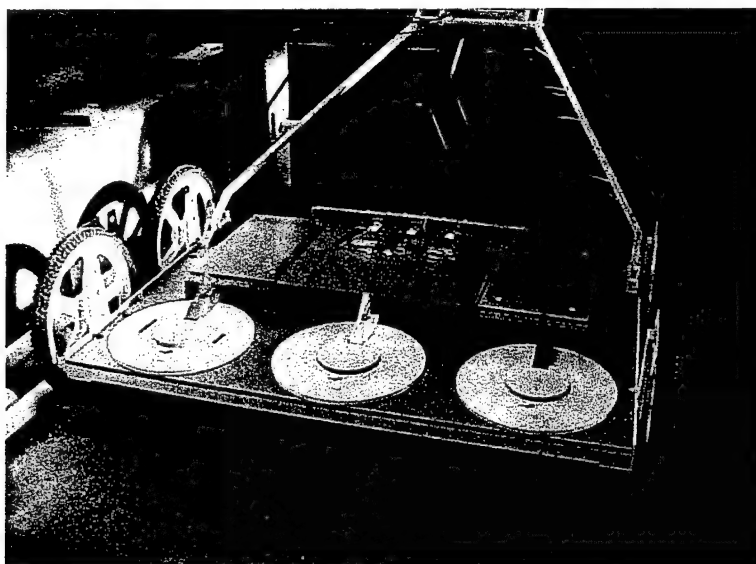


Fig. 10 – Array of GEM-3 sensors for non-synchronous sequential array testing

A positive development for sensor data rate was discovered during the system design phase of this task. The baseline GEM-3 sensor operates on a 1/30 second base period. That is, each sensor acquires data for a multiple of this base period. It then takes approximately two base periods to perform the internal data reduction calculations before the results of the measurement are available to the recording computer. If each of the three sensors in this sequential array are configured to record for a single base period, they can then be run near their maximum rate. The effective sampling rate for the three sensor array is ~9.5 Hz. Coupled with a survey speed of ~3 mph results in a down-track sampling interval of ~15 cm. This results in an acceptable data density for analysis.

As in the case of the individual sensors, the array was calibrated, tested on our test stand, and used to conduct a walking survey over the test field. Details of the calibration results are shown in Figure 11. Each of the sensors in the array was calibrated using a standard chrome sphere mounted on a spacing jig. The results for each of the sensors were compared and plotted over measurements made during the characterization of the baseline GEM-3 sensor. As can be seen in Figure 11, all four of these

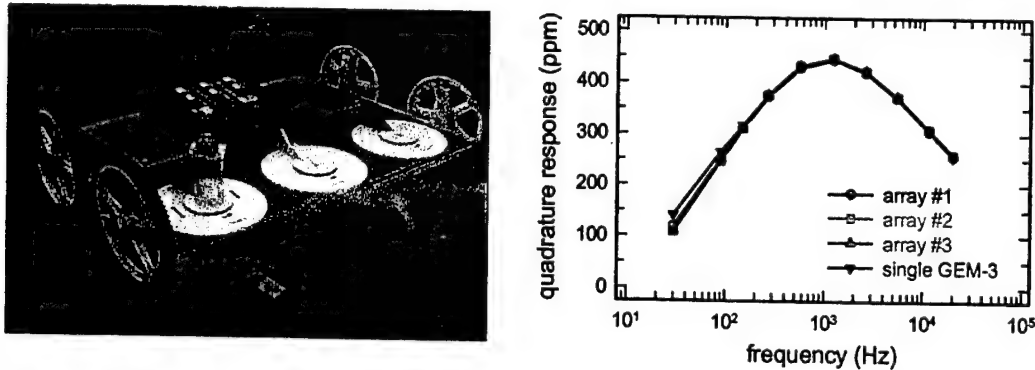


Fig. 11 – Calibration of the individual sensors in the array using a standard chrome sphere (left panel) and comparison of the results with our earlier measurements on an individual sensor (right panel)

measurements agree well. Following calibration, the sensor array was tested on the test stand and over the test grid (Figure 12).

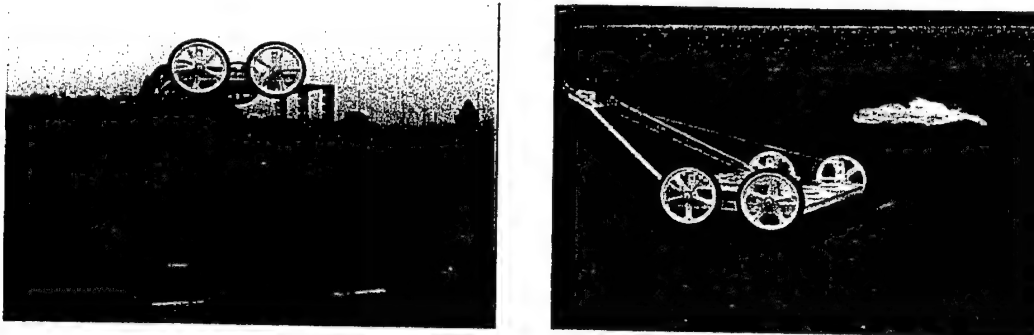


Fig. 12 – Static test stand (left panel) and dynamic survey (right panel) measurements on the GEM-3 array

An unexpected result occurred during the walking survey of the test grid. Figure 13 shows a comparison of the sensor noise at two frequencies for static vs. walking operation. Obviously, the noise at the lowest frequency is more than an order of magnitude higher for the walking survey than the static one. For the higher frequency shown in the plot, which is an intermediate frequency for the GEM sensor, the walking noise is only slightly higher than the static case. Note, however, that there are two targets visible in the intermediate frequency data. Unfortunately, this enhanced noise at the lowest frequencies seriously impacts the classification performance that can be expected from a frequency-domain sensor. Figure 14 is a plot of the peak quadrature frequency vs. the target diameter for transverse and longitudinal excitation of a variety of targets. For any target larger than about 50-mm diameter, frequencies below 100 Hz must be accessible to resolve the peak quadrature frequency. This includes most of the ordnance that will be the targets of the GEM array. Thus, if this noise problem cannot be solved, the GEM sensor array will be of limited value.

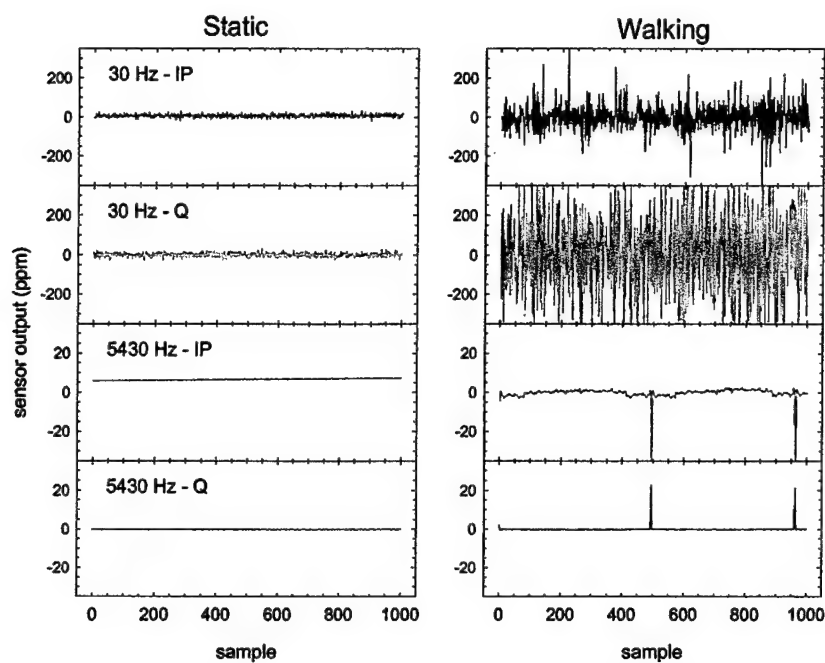


Fig. 13 – Comparison of sensor noise at two frequencies for static vs. walking operation of the GEM array

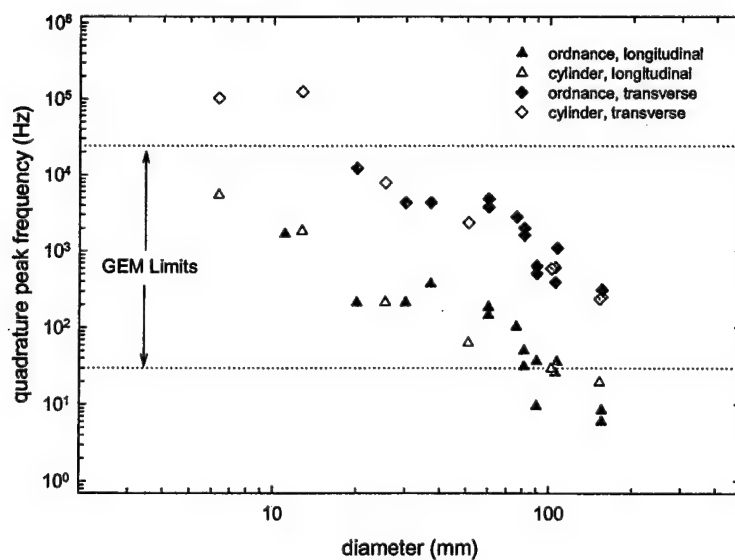


Fig. 14 – Peak frequency of the quadrature response as a function of target diameter for longitudinal and transverse excitation

Array Noise Investigation

Our initial hypotheses on the source of the survey noise in the array centered on acoustic distortion in the coils themselves. The GEM-3 coils are constructed with a relatively light foam base for the windings. This design is intended to make the sensor suitable for hand-carried operation. If coil vibrations had been the source of our observed noise it would have been easy to remedy in our application. With the consent of the ESTCP Program Office, we undertook a three-month investigation of the source and possible remedies for the observed noise.

The first item in this new task was a careful quantification of the magnitude of the noise problem. This task was carried out by Geophex scientists at their Raleigh facility. Figure 15 plots the standard deviation of the observed signal from a GEM-3 as a function of frequency for static and dynamic operation. These results confirm our initial field observations. We will examine these noise measurements in three regimes.

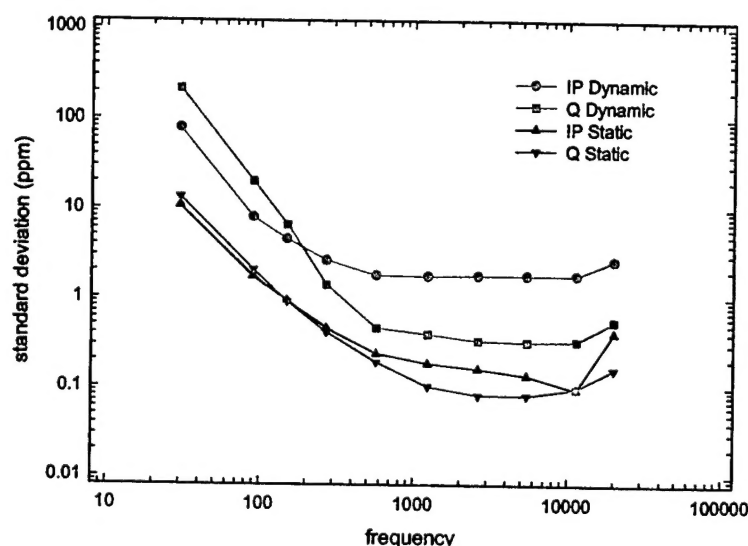


Fig. 15 – Measured noise amplitude as a function of frequency for static and dynamic operation of a GEM-3

At low frequencies (below 300 Hz), the noise in both the in-phase and quadrature components of the response is approximately an order of magnitude larger for dynamic operation. This is the noise that interferes with our classification ability and whose source must be determined. Three sources were investigated: acoustic vibrations that distort the shape of the sensor disk inducing residual bucking error modulation, platform vibration that oscillates the relative position of the metal electronics console relative to the sensor disks, and motion of the receive coil in the earth's magnetic field. A series of tests were performed to isolate each of these noise sources during June and July 2001 at the Geophex facility. The results were quite clear, the only source of noise with an appropriate amplitude and frequency dependence is motion of the receive coil in the earth's field. After the tests, we did a quick back-of-the-envelope calculation to confirm our results. This calculation confirms that a low-frequency rotation of the receive coil in the Earth's field with amplitude of 2° can result in tens of ppm noise in the 30 Hz frequency band.

One can reasonably inquire as to why this low-frequency noise has not manifested itself during the many previous surveys using the GEM-3 in a hand-held mode. The rotational motion of a hand-held GEM-3 is considerably less than on the light-weight, rigid carts used either as a single sensor or on the prototype array. Walking with the hand-held GEM-3 does in fact result in rhythmic bobbing motion, and the corresponding (almost coherent) noise induced in the inphase response over magnetic ground is well documented and has been measured with controlled motion and compared with theory. It is frequency independent and the bouncing vertical motion of the cart determines the inphase noise floor at high frequencies in Figure 15. Rotational motion, however, is not significant in the hand-held GEM-3 surveys (it is rather gentle, probably below 1-2 Hz, and the induced *emf* in the Rx is proportional to rotational rate). The light, rigid cart used for the prototype array, even over a typical lawn, visibly bounces, with each wheel independent of the other, causing rotational motion. Pushing the cart at a fast walking pace (as shown in Figure 10) generates bouncing rotational motion over a greater frequency range than hand-held motion, extending well above 1-2 Hz, with much greater angular rates. As expected, the noise amplitude does increase with decreasing frequency and "side-lobe" leakage is indeed the culprit in terms of data corruption (for the single 30Hz base-period data collected in these tests, the main lobe of the 30Hz correlation extends to DC, so that low-frequency noise actually leaks in through the "flank" of the main lobe).

At higher frequencies, the dynamic quadrature response approaches the static noise level and does not interfere with our classification ability. This noise probably does have a fundamental difference from the lower frequencies. Likely candidates include acoustic vibrations of the platform and/or sensor disk (either creating rotational motion in the Earth's field, similar to the low frequency but not simple rigid body motion, or causing sensor deformations inducing modulation of the residual primary field (imperfect bucking).

Finally, there is still significant noise observed in the in-phase component at high frequencies which results from moving the coil closer and further from the ground as the sensor is walked over the test plot. Unlike the situation at low frequencies, this noise is observed to be coherent across all frequencies (i.e. profile data for all of the frequencies track each other within a percent or two when no metal target is present). This is true for both hand-held and cart mounted GEM-3 surveys, with the former showing rhythmic bobbing undulations coherent with the walking steps of the operator; this effect is in fact reduced when a cart is used, keeping the coil at a constant height, and the effect has been demonstrated to much greater over highly magnetically susceptible terrain. This noise is not a high-frequency effect, it is an all-frequency effect, but at low frequencies is masked by the rotational motion in the Earth's field when on the cart (the vertical motion over magnetic soil remains dominant to much lower frequencies when hand-held).

The high relative noise at low frequencies (again, ppm refers to the fraction of the transmit current that is induced in the receive coil) stems primarily from the low transmit moment of the baseline GEM-3. The sensor was designed for man-portable use where battery weight is a limitation and to detect relatively shallow objects. Neither of these conditions is necessarily valid for a towed array. We have the luxury of large battery reservoirs in the tow vehicle and are thus less limited in transmit moment. Increasing the transmit moment by an order of magnitude will reduce the relative noise the required amount.

SENSOR SPECIFICATION FOR DEMONSTRATION ARRAY

Based on the characterization results detailed above, we have defined the sensors to be used in the *MTADS* GEM array. The coils used in the array will be 96-cm diameter with a larger number of turns. New, higher current electronics have been designed and are being constructed to drive the coils. The product of these two factors will result in the order of magnitude increase in transmit moment discussed above. The new sensor electronics bring other benefits as well. We will now be able to implement real-time low-pass filtering of the induced current using a DSP chip in the receive circuit. This will reduce the absolute level of the noise in addition to the relative decrease from the increased transmit moment. A sketch of the new coils and their planned arrangement in the array is shown in Figure 16.

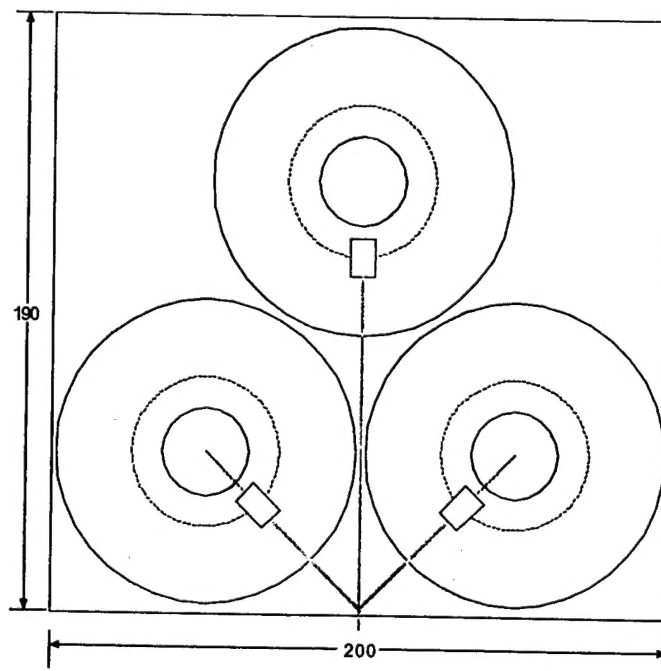


Fig. 16 – Sketch of the arrangement of the custom GEM-3 sensors for the proposed *MTADS* array

Other deployment measures will be taken to reduce the induced noise in the sensor array. The three sensors will be mounted on a rigid honeycomb platform to minimize relative motion. We will optimize the sensor cart for steady ride. This will include making the wheel base as long as possible and experimenting with tire pressure. We also plan to deploy an array of GPS receivers to measure orientation of the sensor platform as well as position. This will give us the ability to post-correct the data for sensor orientation effects.

REFERENCES

1. "Results of the *MTADS* Technology Demonstration #3, Jefferson Proving Ground, Madison, IN," J. R. McDonald, H. H. Nelson, R. Jeffries, and R. Robertson, NRL/PU/6110--99-375, January 1999.
2. "*MTADS* Unexploded Ordnance Operations at the Badlands Bombing Range, Pine Ridge Reservation, Cury Table, SD," J. R. McDonald, H. H. Nelson, J. Neece, R. Robertson, and J. Jeffries, NRL/PU/6110--98-353, July 1997.
3. "Jefferson Proving Ground Technology Demonstration Program Summary," G. Robitaille, J. Adams, C. O'Donnell, and P. Burr, <http://aec.army.mil/usaec/technology/jpgsummary.pdf>.
4. "Electromagnetic Induction Spectroscopy," I. J. Won, D. A. Keiswetter, and E. Novikova, *J. Envir. Eng. Geophysics*, 3, 27 (1998).
5. "Design and Construction of the NRL Baseline Ordnance Classification Test Site at Blossom Point," H. H. Nelson, J. R. McDonald, and R. Robertson, NRL/MR/6110--00-8437, March 2000.
6. "Analysis of GEM Sensor Arrays," R. S. Jones, AETC Report, VA-094-082-TR, June 2000.